Linearly polarized pumped passively Q-switched Nd:YVO_4 microchip laser for Ince–Gaussian laser modes with controllable orientations

2016 J. Opt. 18 125202

(http://iopscience.iop.org/2040-8986/18/12/125202)

IOP Publishing Journal of Optics
J. Opt. 18 (2016) 125202 (10pp) doi:10.1088/2040-8978/18/12/125202

Linearly polarized pumped passively Q-switched Nd:YVO_4 microchip laser for Ince–Gaussian laser modes with controllable orientations

Hong-Sen He[1], Ming-Ming Zhang[1], Jun Dong[1] and Ken-Ichi Ueda[2]

[1] Laboratory of Laser and Applied Photonics (LLAP), Department of Electronics Engineering, School of Information Science and Engineering, Xiamen University, Xiamen 361005, People's Republic of China
[2] Institute for Laser Science, University of Electro-Communications, 1-5-1 Chofugaoka, Chofu, Tokyo 182-8585, Japan

E-mail: jdong@xmu.edu.cn

Received 26 July 2016, revised 3 October 2016
Accepted for publication 19 October 2016
Published 15 November 2016

Abstract

A tilted, linearly polarized laser diode end-pumped Cr^{4+}:YAG passively Q-switched a-cut Nd:YVO_4 microchip laser for generating numerous Ince–Gaussian (IG) laser modes with controllable orientations has been demonstrated by selecting the crystalline orientation of an a-cut Nd:YVO_4 crystal. The same IG laser mode with different orientations has been achieved with the same absorbed pump power in a passively Q-switched Nd:YVO_4 microchip laser under linearly polarized pumping when the incident pump power and the crystalline orientation of an a-cut Nd:YVO_4 crystal are both properly selected. The significant improvement of pulsed laser performance of controllable IG modes has been achieved by selecting the crystalline orientation of an a-cut Nd:YVO_4 crystal. The maximum pulse energy is obtained along the a-axis of an a-cut Nd:YVO_4 crystal and the highest peak power is achieved along the *c*-axis of an a-cut Nd:YVO_4 crystal, respectively, which has potential applications on quantum computation and optical manipulation. The generation of controllable IG laser modes in microchip lasers under linearly polarized pumping provides a convenient and universal way to control IG laser mode numbers with anisotropic crystal as a gain medium.

Keywords: Ince–Gaussian modes, beam characteristics, microchip laser, passively Q-switched, solid-state lasers, linearly polarized pumping

(Some figures may appear in colour only in the online journal)

1. Introduction

The Ince–Gaussian (IG) mode [1] has a much more transverse distribution than the Hermite-Gaussian (HG) mode and Laguerre–Gaussian (LG) mode due to the variable ellipticity of the IG mode. Based on this fact, the applications of IG modes are more diverse and flexible. Recently, extensive studies on IG modes were carried out on optical vortices [2], optical tweezers [3], and optical assembly of microparticles [4]. The IG modes generated in solid-state lasers display a better performance in output power and energy than that generated by modulating the spatial light [5, 6]; this is due to the low damage threshold of the modulators. Various methods are utilized to generate IG modes in solid-state lasers such as tilted pumping [7–9], off-axis pumping [10], introducing an additional cross hair [11] or shaping the pump beam spot by moving a pinhole [12]. The IG mode numbers can be controlled by adjusting some parameters such as incident pump power, pump beam area, tilted angle of pump beam and so on. However, there are a few shortcomings for these methods. For example, there are great losses in pump power by means of shaping the pump beam spot by moving a pinhole [12]. It is

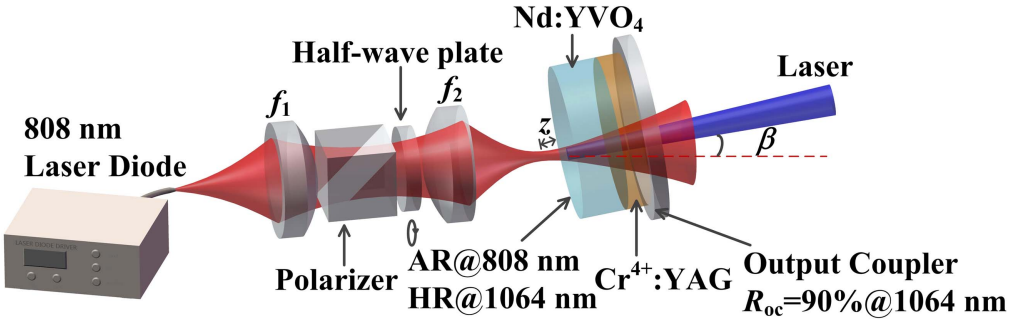

Figure 1. The experimental setup of the polarization dependent microchip laser. f_1 is the collimating lens, f_2 is the focusing lens, β is the tilted angle of the pump beam. z is the distance between the pump beam focus spot and rear surface of the Nd:YVO_4 crystal.

difficult to precisely define the size of the pump beam spot or the distance of the pump spot away from the principal axis in the method of off-axis pumping [10]. It is complicated to adjust the liquid-crystal display to achieve various IG modes due to the complex structure of the liquid-crystal display [5]. Now apart from the method of controlling the pump power incident on the gain medium, there is no other convenient and universal way to change IG mode numbers in lasers. On the other hand, most of the efforts have recently been paid to control the IG mode numbers in solid-state lasers [2, 3, 7–14]. However, the orientation of the IG mode was not taken into account in the solid-state lasers for IG modes. The orientation of the IG mode is one of the significant characteristics of transverse modes and has been used for potential applications. For instance, two major-axis-perpendicular $IG^{o}_{1,1}$ modes with a $\pi/2$ phase difference have been used to generate the donut-like vortex IG mode, $HIG^{\pm}_{1,1}$ [10]. Therefore, desired IG modes with controllable orientations generated in solid-state lasers are required for potential applications on formation of various vortex beams and so on.

The number of IG laser modes increases with the absorbed pump power (P_{abs}) [7]. The absorptivity of the laser crystal is an important factor to decide P_{abs}. The absorption coefficient of anisotropic crystals strongly depends on the crystalline orientations. Hence, the crystalline orientations dependent absorption coefficient of anisotropic crystals such as Nd:YVO_4 crystal has a great effect on P_{abs}, and the oscillation of IG laser modes in microchip lasers is controlled by the crystalline orientation of anisotropic crystal. However, there are no reports on the effect of crystalline orientations of anisotropic crystals on the formation of IG modes in passively Q-switched microchip lasers.

A Nd:YVO_4 crystal is selected as an excellent laser material to study the effect of crystalline orientations of anisotropic crystal on IG laser modes. The anisotropic YVO_4 crystal belongs to the tetragonal crystal system. The c-axis of YVO_4 crystal is four-fold symmetrical and the indistinguishable a-axis and b-axis are perpendicular to the c-axis. The naturally birefringent a-cut Nd:YVO_4 crystal has a characteristic of polarization-dependent absorption coefficient. The absorption coefficient of a-cut Nd:YVO_4 crystal along the extraordinary π direction ($\pi-$polarized, parallel to the c-axis, $\alpha_c = 37\,cm^{-1}$) is 3.7 times of that of the ordinary σ direction ($\sigma-$polarized, parallel to the a-axis, $\alpha_a = 10\,cm^{-1}$) in 1 at.% Nd^{3+} ions doped Nd:YVO_4 crystal at 808 nm [15]. Taking advantages of the polarization-dependent absorption coefficient of an a-cut Nd:YVO_4 crystal, P_{abs} along different crystalline orientations of an a-cut Nd:YVO_4 crystal are different, therefore, different crystalline orientations of Nd:YVO_4 crystal under linearly polarized pumping can generate various different IG laser modes. This method contributes to another convenient and universal way to change IG laser mode numbers in lasers. Meanwhile, it is also an effective way to rotate the orientations of IG laser modes.

In this paper, we studied the effects of the crystalline orientations of an a-cut Nd:YVO_4 crystal on a Cr^{4+}:YAG passively Q-switched a-cut Nd:YVO_4 microchip laser for generating numerous IG laser modes with controllable orientations by tilted, linearly polarized pumping. The same IG laser mode with different orientations have been achieved at the same absorbed pump power when the incident pump power and the crystalline orientation of an a-cut Nd:YVO_4 crystal are both properly selected. The combination effects of the incident pump power and polarization dependent crystalline orientation of an a-cut Nd:YVO_4 crystal on the formation of numerous IG laser modes were investigated systematically. Laser pulses with versatile IG mode distribution and significant improvement of laser performance have been achieved by selecting the crystalline orientation of an a-cut Nd:YVO_4 crystal.

2. Experiments

The experimental setup for tilted, linearly polarized laser diode end-pumped Cr^{4+}:YAG passively Q-switched Nd:YVO_4 microchip laser for generating numerous IG laser modes is shown in figure 1. The parameters of the crystals and the laser diode used in the experiments are the same as those in [9]. Because of the large divergence angle of the output beam from the laser diode, two lenses, f_1 and f_2, were used to shape the pump light in order to effectively pump the gain medium. The focal lengths of the two lenses were 8 mm. A 160 μm-diameter pump beam focus spot was achieved. A Glan-Laser polarizer and a half-wave plate were put between the two lenses to control the polarization of the pump beam. The random polarization of the laser diode was converted to

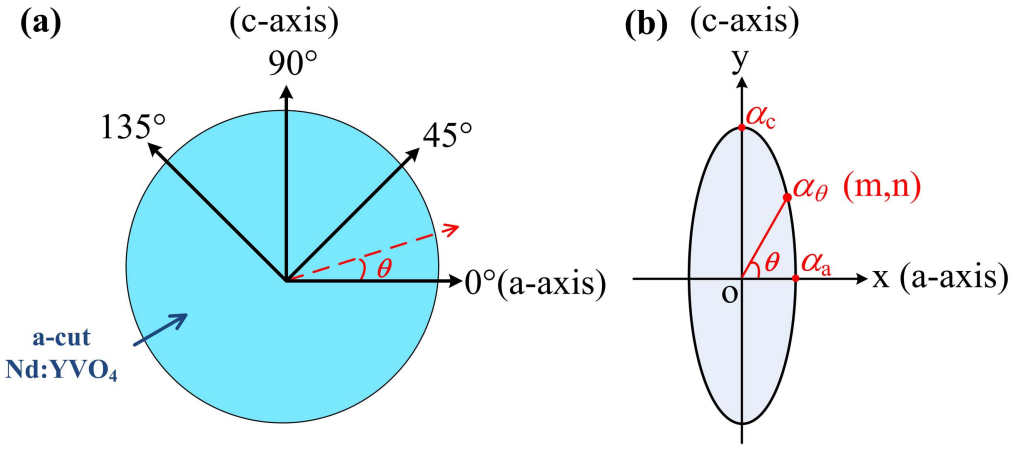

Figure 2. (a) Anisotropic structure of an a-cut Nd:YVO_4 crystal and the four particular crystalline orientations of an a-cut Nd:YVO_4 crystal. θ is the angle between the selected crystalline orientation and the a-axis of the a-cut Nd:YVO_4 crystal. (b) The absorption coefficient of an arbitrary crystalline orientation of a-cut Nd:YVO_4 crystal in terms of the elliptic equation.

linearly polarization by applying a Glan-Laser polarizer. The polarization direction of linearly polarized pump beam was controlled by using a half-wave plate. Based on our previous experimental results and theoretical calculations of the saturated inversion population inside the Nd:YVO_4 crystal as a function the tilted angle of the pump beam [9], the crystals were tilted 3° away from the pump beam direction for obtaining numerous IG modes. The tilted direction of Nd:YVO_4 crystal is along the linearly polarized pump beam direction in the c-a plane of the Nd:YVO_4 crystal. The Nd:YVO_4 crystal was not positioned at the focus spot of pump beam for generating IG modes according to the position dependent high order mode generation in microchip laser [9]. The distance of the Nd:YVO_4 crystal away from the focus spot z was set to be 0.8 mm and the microchip laser was performed at room temperature without cooling devices. A power meter was used to measure the laser power. The output laser properties were measured with an InGaAs photodiode (5 GHz) and a digital oscilloscope (Tektronix, 6 GHz, TDS6604). The beam profiles were observed with a CCD analyzer (BC106-VIS, Thorlabs).

3. Results and discussion

Figure 2 shows the anisotropic structure of the a-cut Nd:YVO_4 crystal, and the relationship between linearly polarized pump beam and the crystalline orientation of an a-cut Nd:YVO_4 crystal. θ is the angle between the selected crystalline orientation and the a-axis of a Nd:YVO_4 crystal. $\theta = 0°$ and $\theta = 90°$ denote to the a-axis and c-axis of an a-cut Nd:YVO_4 crystal, respectively. Four particular crystalline orientations (0°, 45°, 90° and 135°) of an a-cut Nd:YVO_4 crystal were selected to study the effects of the crystalline orientations of the a-cut Nd:YVO_4 crystal on the microchip laser under linearly polarized pumping for generating various IG modes. These four particular crystalline orientations of a Nd:YVO_4 crystal could essentially represent all the crystalline orientations due to the four-fold symmetrical structure of Nd:YVO_4 crystal.

P_{abs} has a great effect on the IG laser mode oscillations in the laser cavity [7]. P_{abs} of an a-cut Nd:YVO_4 crystal strongly depends on the crystalline orientation; this is because the absorption spectrum of Nd:YVO_4 crystals is a polarization dependent absorption spectrum. The polarization dependent P_{abs} of the Nd:YVO_4 crystal as a function of the incident pump power (P_{in}) and crystalline orientation dependent absorption coefficient (α_θ) can be expressed as:

$$P_{abs} = P_{in}[1 - \exp(-\alpha_\theta \cdot l)] \quad (1)$$

where l is the length of a-cut Nd:YVO_4 crystal, α_θ is the absorption coefficient of laser medium along different crystalline orientations (θ) of an a-cut Nd:YVO_4 crystal. Figure 2(b) shows the absorption coefficient within an arbitrary crystalline orientation of an a-cut Nd:YVO_4 crystal. The absorption coefficient was defined in terms of the elliptic equation, $m^2/{\alpha_a}^2 + n^2/{\alpha_c}^2 = 1$, where (m, n) is the coordinate of an arbitrary crystalline orientation on the ellipse, where α_a and α_c are the absorption coefficients along the a- and c-axes of an a-cut Nd:YVO_4 crystal, respectively. Besides, $n/m = \tan(\theta)$ and ${\alpha_\theta}^2 = m^2 + n^2$. Therefore, the value of α_θ is assumed to be

$$\alpha_\theta = \frac{\alpha_a \cdot \alpha_c}{\sqrt{\alpha_a^2 \cdot \sin^2(\theta) + \alpha_c^2 \cdot \cos^2(\theta)}}. \quad (2)$$

The absorption coefficient of a-cut Nd:YVO_4 crystals strongly depends on the crystalline orientation. From equation (1), it can be found that P_{abs} is not only determined by P_{in} but also governed by the crystalline orientations of the Nd:YVO_4 crystal.

Figure 3 shows the theoretically calculated P_{abs} as a function of crystalline orientation (θ) of an a-cut Nd:YVO_4 crystal for different P_{in}. The 1 mm-thick Nd:YVO_4 crystal was used in this calculation. P_{abs} increases with the crystalline orientation (θ) when the a-cut Nd:YVO_4 crystal is rotated from the a-axis anti-clockwise to the c-axis, and then decreases with θ when the a-cut Nd:YVO_4 crystal is rotated from the c-axis anti-clockwise to the a-axis. There is a

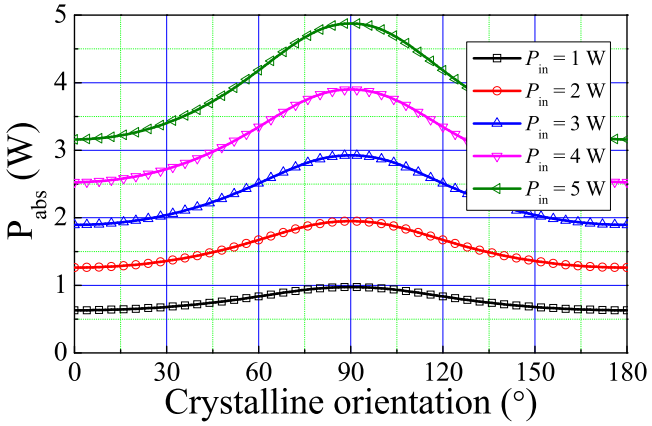

Figure 3. The theoretically calculated absorbed pump power as a function of crystalline orientation (θ) of a-cut Nd:YVO_4 crystal for different P_{in}.

maximum P_{abs} at the *c*-axis of a Nd:YVO_4 crystal, $\theta = 90°$ for different P_{in}. P_{abs} increases with P_{in} for a certain crystalline orientation. The same P_{abs} could be obtained by properly selecting P_{in} and the crystalline orientation of an a-cut Nd:YVO_4 crystal under linearly polarized pumping. For instance, when P_{in} is set to 4 W, 3.5 W absorbed pump power can be achieved with linearly polarized pump beam parallel to the crystalline orientation of 66°. 3.5 W absorbed pump power can also be achieved with $P_{in} = 5$ W and the linearly polarized pump beam parallel to the crystalline orientation of 36°.

The polarization direction of the linearly polarized pump beam is chosen to parallel the four crystalline orientations of the Nd:YVO_4 crystal ($\theta = 0°$, 45°, 90° and 135°) to study the effect of crystalline orientation on the formation of IG modes in microchip lasers. Figure 4(a) shows the evolution of a typical experimentally observed IG laser mode distribution in passively Q-switched Nd:YVO_4 microchip laser with P_{in} for four crystalline orientations under linearly polarized pumping. The corresponding numerical simulations of experimentally observed IG laser modes are shown in figure 4(b). The experimentally obtained IG laser modes were numerically simulated to confirm the mode indices according to the IG mode theoretical formula [1].

The IG laser mode number increases with P_{in} for different crystalline orientations of a-cut Nd:YVO_4 crystals when P_{in} is higher than the lasing threshold. The IG laser mode numbers generated in microchip lasers strongly depend on P_{in} for a certain crystalline orientation of the a-cut Nd:YVO_4 crystal. When the pump polarization direction is parallel to the a-axis of an a-cut Nd:YVO_4 crystal ($\theta = 0°$), the absorbed pump power is low for different P_{in}, as shown in figure 3. Therefore, the threshold of P_{in} for laser oscillation is 1.55 W. TEM_{00} mode laser oscillates when P_{in} is less than 2.1 W. $IG^{o}_{1,1}$ mode laser oscillates when P_{in} increases from 2.1 W to 2.5 W. When P_{in} is set between 2.5 W and 3 W, $IG^{o}_{2,0}$ mode laser oscillates. $IG^{o}_{5,5}$ mode laser oscillates when P_{in} increases from 3 W to 3.5 W. $IG^{e}_{7,3}$ mode laser oscillates with further increasing of P_{in}.

The oscillation of different IG laser modes in passively Q-switched Nd:YVO_4 microchip laser depends on the spatial saturated inversion population distribution inside the gain medium. The saturated inversion population increases with the incident pump power for a certain crystalline orientation of Nd:YVO_4 crystal under linearly polarized pumping. When the inversion population around the edge regions of the pump area inside the Nd:YVO_4 crystal was increased high enough to overcome the cavity loss, the laser cavity supported the oscillation of a higher order IG laser mode. In that case, the competition occurred between the two IG laser modes for extracting the energy stored in the inversion population provided by P_{in}. The higher order IG laser mode had a larger oscillation region inside the Nd:YVO_4 crystal than the former one. Therefore, due to the higher overlap efficiency between the oscillation region of the higher order IG laser mode and pump region, the higher order IG laser mode fully extracted the energy stored in the inversion population inside the Nd:YVO_4 crystal and started to oscillate, and the former IG laser mode could not lase. For example, when P_{in} was increased from 3 W to 3.5 W ($\theta = 0°$), the $IG^{o}_{5,5}$ mode laser oscillated rather than the $IG^{o}_{2,0}$ mode, owing to the larger oscillation region of $IG^{o}_{5,5}$ laser mode inside the Nd:YVO_4 crystal.

When the pump polarization direction was set between the a- and *c*-axes of an a-cut Nd:YVO_4 crystal ($\theta = 45°$ or $\theta = 135°$), P_{abs} increases and the threshold of P_{in} is decreased to 1.47 W for $\theta = 45°$. The TEM_{00} fundamental mode laser oscillates when P_{in} is above the lasing threshold and until up to 2 W. $IG^{o}_{1,1}$ mode laser oscillates when P_{in} is within the range from 2 W to 2.2 W. The $IG^{e}_{2,0}$ mode laser oscillates when P_{in} is within 2.2 W and 2.5 W. The $IG^{o}_{4,0}$ mode laser oscillates when P_{in} is in the range from 2.5 W to 3 W. The $IG^{o}_{8,8}$ and TEM_{00} modes oscillate simultaneously when P_{in} increases from 3 W to 3.5 W. Whereas the $IG^{e}_{10,10}$ and TEM_{00} modes oscillate simultaneously when P_{in} is higher than 3.5 W. Similar laser modes were observed when the pump polarization direction is parallel to 135° of the Nd:YVO_4 crystal. The incident pump power threshold of 1.45 W for $\theta = 135°$ is nearly the same at that for $\theta = 45°$. The slight difference between laser modes when P_{in} is higher than 2.5 W may be attributed to the adjustment errors of optical elements.

When the pump polarization direction was set to parallel the *c*-axis of the a-cut Nd:YVO_4 crystal ($\theta = 90°$), P_{abs} increases and the threshold of P_{in} for laser oscillation is decreased to 1.35 W. The TEM_{00} fundamental mode laser oscillates when P_{in} is higher than the incident pump power threshold. The $IG^{o}_{1,1}$ mode laser oscillates when P_{in} increases up to 1.8 W. The $IG^{o}_{2,2}$ mode laser oscillates when P_{in} is in the range from 1.9 W to 2.2 W. The $IG^{o}_{3,1}$ mode laser oscillates when P_{in} is higher than 2.2 W. The $IG^{e}_{3,3}$ mode laser oscillates when P_{in} is within 2.5 W and 3 W. The $IG^{e}_{10,10}$ and TEM_{00} fundamental modes oscillate simultaneously when P_{in} is in the range of 3 to 3.5 W. The $IG^{e}_{11,11}$ and TEM_{00} fundamental modes oscillate when P_{in} is higher than 3.5 W.

As shown in figure 4, crystalline orientations of an a-cut Nd:YVO_4 crystal not only determines the IG laser mode generated, but also has an obvious effect on the major axis of IG laser modes. When the pump polarization direction is

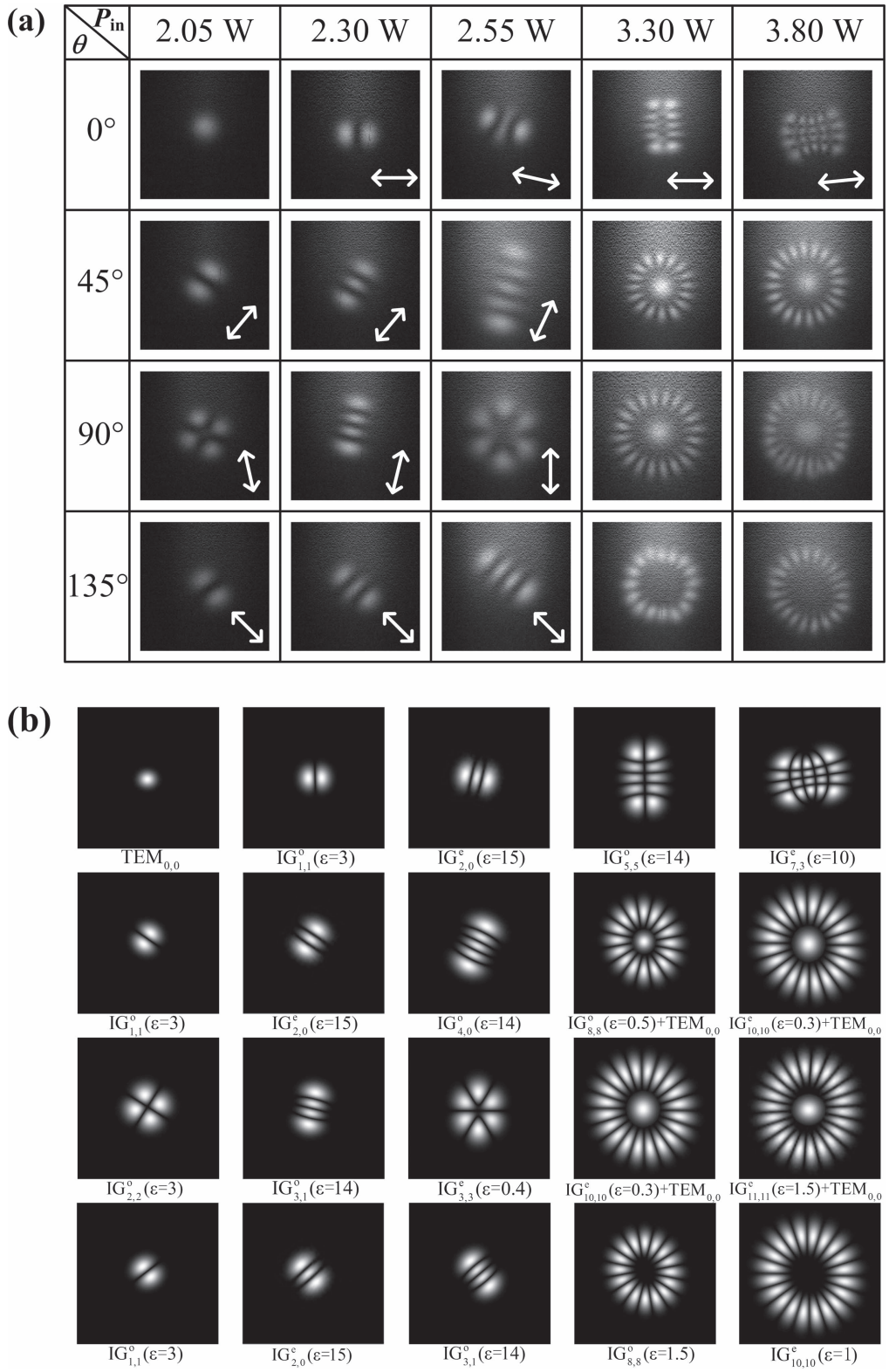

Figure 4. (a) The typical experimentally observed IG laser mode distribution for four crystalline orientations under linearly polarized pumping in Cr^{4+}:YAG passively Q-switched a-cut Nd:YVO_4 microchip laser at different incident pump powers. The arrows denote the directions of the major axes of the IG laser modes. θ was set to be 0°, 45°, 90° and 135°. P_{in} was set to be 2.05 W, 2.3 W, 2.55 W, 3.3 W and 3.8 W. (b) The corresponding numerically simulated IG laser modes obtained in figure 4(a).

parallel to the *a*-axis of an a-cut Nd:YVO_4 crystal ($\theta = 0°$), the major axes of the IG laser modes were nearly horizontal. When the pump polarization direction is parallel to 45° of the Nd:YVO_4 crystal, the major axes of the IG laser modes also rotated about 45°. The major axes of the IG laser modes were almost perpendicular to the horizontal line when the pump polarization direction was parallel to the *c*-axis of the a-cut Nd:YVO_4 crystal ($\theta = 90°$). The major axes of the IG laser modes were rotated 135° when the pump polarization direction was rotated 135° to be set between the *c*-axis and a-axis of the a-cut Nd:YVO_4 crystal. In other words, the major axis of the IG laser modes generated linearly polarized pumped passively Q-switched Nd:YVO_4 microchip lasers that can be controlled by the crystalline orientation of an a-cut Nd:YVO_4 crystal. Because the P_{abs} inside a Nd:YVO_4 crystal increases when the pump polarization direction is not parallel to the a-axis of a Nd:YVO_4 crystal, the saturated inversion population distribution under high pump power level tends to be smooth inside the Nd:YVO_4 crystal. Therefore, the major axes of IG laser modes with relative small ellipticity at high pump power are indistinct.

It is found that the same IG laser mode generated in microchip laser at the same P_{in} when the pump polarization direction is parallel to 45° and 135° of a-cut Nd:YVO_4 crystal, as shown in figure 4. $IG^{o}_{1,1}$ laser mode and $IG^{e}_{2,0}$ laser mode were generated at $P_{in} = 2.05$ W and 2.30 W for $\theta = 45°$ and $\theta = 135°$ of a-cut Nd:YVO_4 crystal, respectively. The direction of the major axis of these generated IG mode at the same P_{in} for $\theta = 45°$ and $\theta = 135°$ of a-cut Nd:YVO_4 crystal is perpendicular each other. This is attributed to symmetrical orientation in the tetragonal structure of Nd:YVO_4 crystal when the pump polarization direction lays between a-axis and *c*-axis of a-cut Nd:YVO_4 crystal (e.g. $\theta = 45°$ and $\theta = 135°$). The P_{abs} for $\theta = 45°$ and $\theta = 135°$ is the same at the same P_{in} applied.

Besides the similar IG laser modes generated for the same P_{in} when the pump polarization direction was set to be parallel to the crystalline orientations at $\theta = 45°$ and $\theta = 135°$ of an a-cut Nd:YVO_4 crystal, the same IG laser modes have been obtained when the P_{abs} is coincident by properly selecting the crystalline orientation of an a-cut Nd:YVO_4 crystal to be within the pump polarization direction and applying suitable P_{in}. The $IG^{o}_{1,1}$ laser mode with different major axis directions have been generated at $P_{abs} = 1.31$ W for $P_{in} = 2.3$ W and $\theta = 0°$, $P_{in} = 2.05$ W and $\theta = 45°$ and 135°. The $IG^{e}_{2,0}$ laser mode with different major axis directions was also obtained at $P_{abs} = 1.55$ W for $P_{in} = 2.55$ W and $\theta = 0°$, $P_{in} = 2.3$ W and $\theta = 45°$ and 135°. The $IG^{0}_{3,1}$ laser modes with different major axis directions were obtained at $P_{abs} = 1.76$ W for $P_{in} = 2.3$ W and $\theta = 90°$, as well as $P_{in} = 2.55$ W and $\theta = 135°$. The IG laser modes were all $IG^{e}_{10,10} + TEM_{00}$ with indistinct major axes due to their relatively small ellipticity ($\varepsilon = 0.3$), and they also had the same $P_{abs} = 2.72$ W. Generally speaking, when the pump polarization direction was rotated from 0° to 135°, the major axes of the IG laser modes were also rotated from 0° to 135° with respect to the horizontal line. When P_{in} and the pump polarization direction are both properly selected, the same P_{abs} is achieved to force the same IG laser mode oscillation with different orientations. The same IG laser modes with different major axis directions were generated in passively Q-switched Nd:YVO_4 microchip laser by applying a linearly polarized pump beam to expand the flexibilities for applications of IG laser beams. Therefore, combining the position dependent high order transverse laser mode generation in microchip laser [9], the results of generation of IG modes with controllable orientations provide a novel method for generating LG and HG transverse modes with controllable orientations in passively Q-switched microchip lasers.

The IG laser mode oscillation in microchip lasers are determined by the initial inversion population (N_i) needed and the inversion population distribution (ΔN) provided by the pump power. The spatial distribution of the saturated inversion population (N_{sat}) inside the Nd:YVO_4 crystal along different crystalline orientations in Nd:YVO_4 passively Q-switched laser under tilted beam pumping has been calculated according to the formula from [9] by taking into account the crystalline orientation dependent absorption coefficient of the Nd:YVO_4 crystal. It is found that P_{in} and the tilted angle of pump beam directly determine ΔN when the crystalline orientation is set along the linearly polarized pump beam. The distribution of N_{sat} along the laser propagation direction and the radial direction inside a 1 mm-thick a-cut Nd:YVO_4 crystal for different crystalline orientations under linearly polarized pumping is shown in figure 5. The incident pump power is 3.8 W. $d = 0$ means the position of the rear surface of the Nd:YVO_4 crystal. The N_{sat} with a local minimum on the light axis decreases with d (from 0 to 1 mm) for different crystalline orientations of an a-cut Nd:YVO_4 crystal under linearly polarized pump beam pumping. As shown in figure 5(a)–(b), namely, for $d < 0.4$ mm, the distribution of N_{sat} greatly increases and tends to be broadened with the crystalline orientation of the Nd:YVO_4 crystal, θ. The highest distribution of N_{sat} inside the Nd:YVO_4 crystal contributes to the effect of the gain guiding for generating high-order IG mode [16, 17]. For $d = 0.4$ mm in figure 5(c), the distribution of N_{sat} tends to be the same for different crystalline orientations of the a-cut Nd:YVO_4 crystal. For $d > 0.4$ mm in figures 5(d)–(f), the distribution of N_{sat} decreases with θ. The N_{sat} at $d > 0.4$ mm is much less than at $d < 0.4$ mm. This is caused by the exponential decay of the absorbed pump power inside the Nd:YVO_4 crystal. The spatial distribution of the saturated inversion population is proportional to the inversion population provided by the pump power and is inversely proportional to the intracavity laser intensity. The inversion population is proportional to the incident pump power and is affected by the absorption coefficient and length of Nd:YVO_4 crystal. The inversion population provided by the pump power decreases exponentially with the thickness of the Nd:YVO_4 crystal. Therefore, when the crystalline orientation of the Nd:YVO_4 crystal is set, the saturated inversion population decreases with the position (d) of the Nd:YVO_4 crystal. For a certain absorption coefficient of a Nd:YVO_4 crystal, the inversion population decreases dramatically with d when d is less than 0.4 mm owing to the exponential decay of the absorbed pump power. Therefore, there is a sharp change of

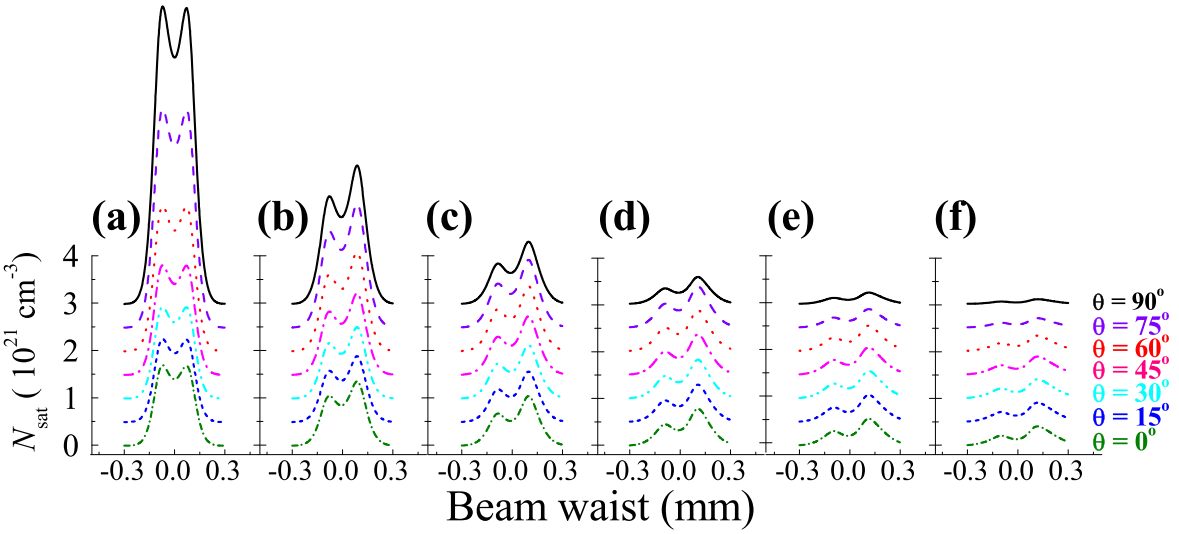

Figure 5. The distribution of saturated inversion population along the laser propagation direction and the radial direction inside a 1 mm-thick a-cut Nd:YVO_4 crystal for different crystalline orientations of a-cut Nd:YVO_4 crystal (θ) under linearly polarized pumping. (a) $d = 0$, (b) $d = 0.2$ mm, (c) $d = 0.4$ mm, (d) $d = 0.6$ mm, (e) $d = 0.8$ mm, (f) $d = 1$ mm. $d = 0$ means the position of the rear surface of the Nd:YVO_4 crystal.

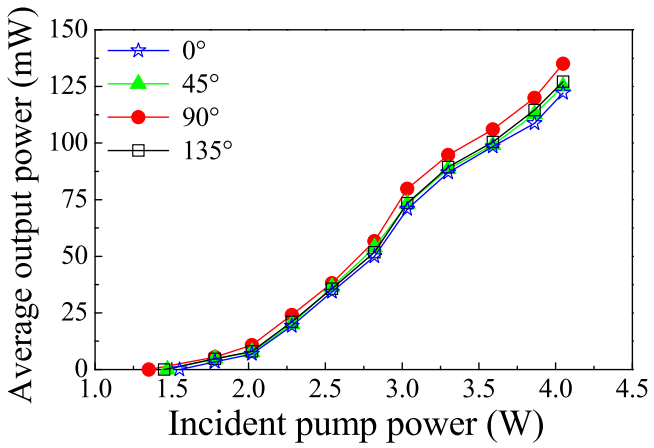

Figure 6. The variation of average output power as a function of P_{in} for four crystalline orientations of Nd:YVO_4 crystal in Cr^{4+}:YAG passively Q-switched a-cut Nd:YVO_4 microchip laser.

the saturated population inversion spatially $d = 0.4$ mm. The distribution of N_{sat} at $d < 0.4$ mm is a dominant factor to determine the total ΔN in Nd:YVO_4 crystals for different crystalline orientations of an a-cut Nd:YVO_4 crystal. Therefore, the mode number of the IG laser mode increases with θ from 0° to 90° owing to the increasing and broadening distributions of N_{sat} inside the a-cut Nd:YVO_4 crystal.

The variation of average output power (P_{out}) as a function of P_{in} for four crystalline orientations of a Nd:YVO_4 crystal in Cr^{4+}:YAG passively Q-switched a-cut Nd:YVO_4 crystal microchip laser is shown in figure 6. The lasing thresholds of P_{in} for the crystalline orientations of 0°, 45°, 90° and 135° were 1.55 W, 1.47 W, 1.35 W and 1.45 W, respectively. The lasing threshold for $\theta = 90°$ was the lowest due to the largest P_{abs} along the c-axis of a-cut Nd:YVO_4 crystal. The lasing threshold for $\theta = 0°$ was the highest owing to the lowest P_{abs} along the a-axis of the a-cut Nd:YVO_4 crystal. The thresholds of P_{in} for $\theta = 45°$ and $\theta = 135°$ are comparable due to the symmetrical crystal structure of an a-cut Nd:YVO_4 crystal. The P_{out} increases linearly with P_{in} for four crystalline orientations of a Nd:YVO_4 crystal when P_{in} is well above the pump power threshold. Maximum P_{out} of 135 mW was achieved at $P_{in} = 4.05$ W for $\theta = 90°$. The P_{out} increased with θ from 0° to 90°, then decreased from 90° to 135° at a certain P_{in}, which was attributed to the variations of P_{abs} with the crystalline orientations of a Nd:YVO_4 crystal. The P_{out} was almost the same for the crystalline orientations of 45° and 135° at a certain P_{in} due to the their symmetrical positions in the tetragonal structure of the Nd:YVO_4 crystal. The wavelength of the output laser was at 1064 nm for four crystalline orientations of a-cut Nd:YVO_4 crystal under linearly polarized pump beam pumping.

The polarization states of the output laser have been measured and found that the linearly polarized laser beam was generated in the Cr^{4+}:YAG passively Q-switched Nd:YVO_4 microchip laser. The output laser was linearly polarized along the c-axis of the a-cut Nd:YVO_4 crystal for different crystalline orientations of a Nd:YVO_4 crystal. In other words, the polarization directions of the output lasers were the same for various IG modes. The extinction ratio of the linearly polarized laser was measured to be larger than 100:1.

Figure 7 shows the variation of the repetition rate, pulse width, pulse energy and peak power as a function of P_{in} for four crystalline orientations of a Nd:YVO_4 crystal in Cr^{4+}:YAG passively Q-switched a-cut Nd:YVO_4 crystal microchip laser. The repetition rate increases with P_{in} for four crystalline orientations of a Nd:YVO_4 crystal and it also increases with θ (from 0° to 90°) under different P_{in}, as shown in figure 7(a). The repetition rate has nearly the same variation tendency with P_{in} for the crystalline orientations of 45° and 135°, which is due to the symmetrical positions in the tetragonal structure of the a-cut Nd:YVO_4 crystal. The repetition rate increases slowly with P_{in} for different crystalline orientations when P_{in} is higher than 2 W. This may be caused by the

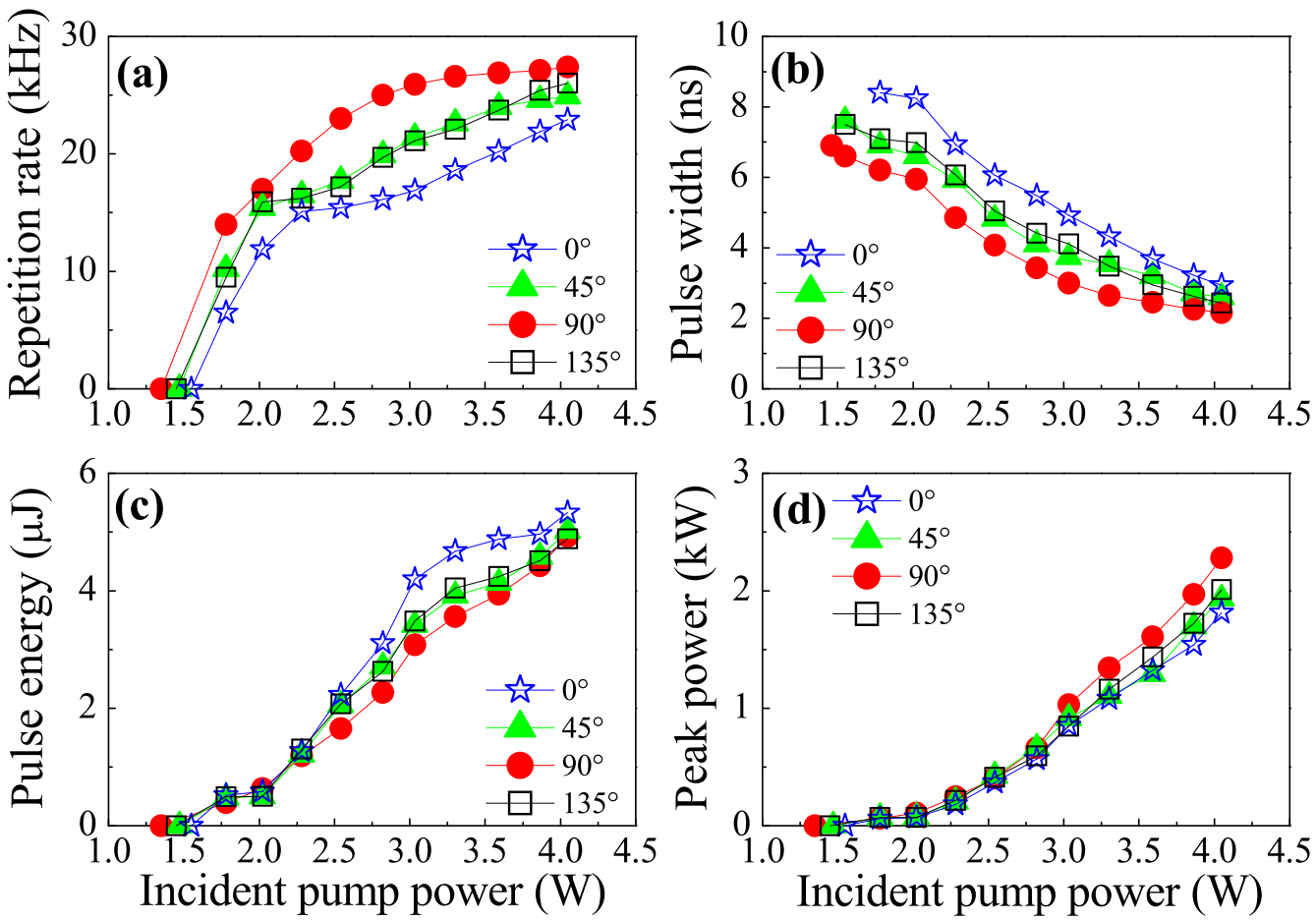

Figure 7. The variation of repetition rate, pulse width, pulse energy and peak power as a function of P_{in} under the four crystalline orientations of Nd:YVO_4 crystal in Cr^{4+}:YAG passively Q-switched a-cut Nd:YVO_4 crystal microchip laser.

higher-order IG mode oscillation with a large laser beam area [18] or thermal effect [19] of Nd:YVO_4 crystal at high pump power. The repetition rate of passively Q-switched laser is determined by the inversion population provided by the pump power, initial inversion population and final inversion population for the laser pulse [20]. The initial and final inversion population after pulse output are determined by the initial transmission of the saturable absorber, which are unchanged when the saturable absorber is fully beached. The inversion population provided by the pump power depends on the pump beam area, incident pump power and thermal effect. The inversion population increases with the incident pump power when the incident pump power is less than 2 W, therefore, the repetition rate increases linearly with the incident pump power. The effective laser beam area increases for high order IG mode oscillation when the incident pump power is high enough to provide the inversion population extended for laser oscillation. The effective inversion population increases slowly owing to the gain guiding effect [16, 17] for laser oscillation in the large pump area, the thermal effect also degrades the inversion population, therefore, the repetition rate increases slowly with the incident pump power. The highest repetition rate of 27.4 kHz was obtained at $P_{in} = 4.05$ W for $\theta = 90°$. The pulse width decreases with P_{in} for different crystalline orientations of a Nd:YVO_4 crystal and the pulse width also decreases with θ (from 0° to 90°) under certain P_{in}, as shown in figure 7(b). The pulse width tends to be constant when P_{in} is greater than 3.55 W. The variation of the pulse width with P_{in} for $\theta = 45°$ is similar to that for $\theta = 135°$ owing to the same P_{abs} for the symmetrical crystal structure of the Nd:YVO_4 crystal. The shortest pulse width of 2.2 ns was achieved at $P_{in} = 4.05$ W for $\theta = 90°$, which was only a quarter of that obtained at randomly polarized pumping [9].

As shown in figure 7(c), the pulse energy increases with P_{in} for different crystalline orientations of a Nd:YVO_4 crystal. However, the pulse energy decreases with θ (from 0° to 90°) under certain P_{in}. The pulse energy has nearly the same variation tendency. A maximum pulse energy of 5.3 μJ was achieved at $P_{in} = 4.05$ W for $\theta = 0°$, which was about 2.5 times higher than that obtained under randomly polarized pumping [9]. As shown in figure 7(d), the peak power increases with P_{in} for different crystalline orientations of Nd:YVO_4 crystal and the peak power increases with θ (from 0° to 90°) under certain P_{in}. The peak power has nearly the same variation tendency for crystalline orientations of 45° to 135°. The highest peak power of 2.3 kW was achieved at $P_{in} = 4.05$ W for $\theta = 90°$, which was about 10.5 times higher than that generated under randomly polarized pumping [9]. The almost linear increase of the output pulse energy and

the peak power with P_{in} for different crystalline orientations of Nd:YVO_4 crystal is due to the high order IG mode oscillation with a large beam area under the gain guiding effect. The thermal lens effect also contributes to the linear increase of pulse energy with P_{in}. The thermal lens effect causes the ratio of the effective area in the laser crystal and in the saturable absorber increases with P_{in} [19]. The enlarged effective laser pumped area for high order IG mode oscillation causes the slow increase of the intracavity laser intensity, which is not high enough to fully bleach the saturable absorber, thus, the pulse energy increases linearly with the incident pump power. Owing to the slow decrease in the pulse width with the incident pump power, the same tendency occurrs for the peak power of the passively Q-switched microchip laser.

When P_{in} is greater than 2.5 W, it is evident to find that the a-axis of an a-cut Nd:YVO_4 crystal under linearly polarized pumping can store more energy in the upper energy level, therefore, the laser pulse processes a higher pulse energy and a lower repetition rate. On the contrary, the high-gain *c*-axis of an a-cut Nd:YVO_4 crystal is able to compress the pulse width and obtain higher peak power. Obviously, compared with randomly polarized pumping, different crystalline orientations of an a-cut Nd:YVO_4 crystal under linearly polarized pumping have great effects on the repetition rate, pulse width, pulse energy and peak power of passively Q-switched Nd:YVO_4 microchip laser. The laser pulse width has been effectively compressed, the pulse energy and peak power have been dramatically improved in passively Q-switched Nd:YVO_4 microchip laser by properly selected crystalline orientation of the Nd:YVO_4 crystal under linearly polarized pumping. A controllable IG mode laser with peak power of over kilowatts and nanosecond pulse width generated a polarization dependent passively Q-switched Nd:YVO_4 microchip laser under linearly polarized pumping; this was found to provide an effective and convenient method for developing high peak power, as well as controllable IG mode laser, which have potential applications on microparticle manipulation and quantum computation. For example, IG mode laser beams with low P_{out} and high peak power can be used in manipulating living cells with high efficiency and less damage.

4. Conclusions

A tilted, linearly polarized laser diode end-pumped Cr^{4+}:YAG passively Q-switched an a-cut Nd:YVO_4 microchip laser for generating numerous Ince–Gaussian (IG) laser modes with controllable orientations has been investigated by selecting the crystalline orientation of an a-cut Nd:YVO_4 crystal. The absorbed pump power distributions inside the Nd:YVO_4 crystal under different crystalline orientations of a Nd:YVO_4 crystal determines the oscillation of numerous IG laser modes with different orientations. The same absorbed pump power is achieved to force the same IG laser mode oscillation when the incident pump power and the crystalline orientation of an a-cut Nd:YVO_4 crystal are both properly selected. IG laser modes with different major axis directions have been generated in microchip lasers under linearly polarized pumping by controlling the crystalline orientation of a Nd:YVO_4 crystal and the incident pump power. The polarization dependent passively Q-switched Nd:YVO_4 microchip laser provides an effective and convenient method for developing high peak power laser with more precise control of the number and orientation of IG laser mode. Various high order IG laser modes with significant improvement of laser performance under properly selected crystalline orientations provide a more flexible and simple method for developing high peak power passively Q-switched laser with controllable IG modes for potential applications on microparticle manipulation and quantum computation.

Acknowledgments

This work was supported by the National Natural Science Foundation of China (61475130 and 61275143), the Program for New Century Excellent Talents in University (NCET-09-0669), and the Fundamental Research Funds for Xiamen University (20720162005).

References

[1] Bandres M A and Gutiérrez Vega J 2004 Ince-Gaussian beams *Opt. Lett.* **29** 144–6
[2] Otsuka K and Chu S C 2009 Generation of vortex array beams from a thin-slice solid-state laser with shaped wide-aperture laser-diode pumping *Opt. Lett.* **34** 10–2
[3] Chu S C, Yang C S and Otsuka K 2008 Vortex array laser beam generation from a Dove prism-embedded unbalanced Mach-Zehnder interferometer *Opt. Express* **16** 19934–49
[4] Woerdemann M, Alpmann C and Denz C 2011 Optical assembly of microparticles into highly ordered structures using Ince-Gaussian beams *Appl. Phys. Lett.* **98** 111101
[5] Bentley J B, Davis J A, Bandres M A and Gutiérrez Vega J C 2006 Generation of helical Ince-Gaussian beams with a liquid-crystal display *Opt. Lett.* **31** 649–51
[6] Ren Y X, Fang Z X, Gong L, Huang K, Chen Y and Lu R D 2015 Dynamic generation of Ince-Gaussian modes with a digital micromirror device *J. Appl. Phys.* **117** 133106
[7] Dong J, Ma J, Ren Y Y, Xu G Z and Kaminskii A A 2013 Generation of Ince-Gaussian beams in highly efficient, nanosecond Cr,Nd:YAG microchip lasers *Laser Phys. Lett.* 10085803
[8] Dong J, He Y, Zhou X and Bai S C 2016 Highly efficient, versatile, self-Q-switched, high-repetition-rate microchip laser generating Ince-Gaussian modes for optical trapping *Quantum Electron.* **46** 218
[9] Dong J, Bai S C, Liu S H, Ueda K I and Kaminskii A A 2016 A high repetition rate passively Q-switched microchip laser for controllable transverse laser modes *J. Opt.* **18** 055205
[10] Chu S C and Otsuka K 2007 Stable donutlike vortex beam generation from lasers with controlled Ince-Gaussian modes *Appl. Opt.* **46** 7709–19
[11] Schwarz U T, Bandres M A and Gutiérrez Vega J C 2004 Observation of Ince-Gaussian modes in stable resonators *Opt. Lett.* **29** 1870–2

[12] Han S, Liu Y Q, Zhang F, Zhou Y, Wang Z P and Xu X G 2015 Direct generation of subnanosecond Ince-Gaussian modes in microchip laser *IEEE Photonics J.* **7** 1–6
[13] Otsuka K 2012 Polarization-dependent intensity noise in a microchip solid-state laser with spatially coherent polarization vector fields *Opt. Lett.* **37** 4287–9
[14] Otsuka K, Chen Y T, Chu S C, Lin C C and Ko J Y 2011 Chaotic oscillations associated with the breakup of polarization entangled coherent states in a microchip solid-state laser *Opt. Lett.* **36** 960–2
[15] Brignon A, Feugnet G, Huignard J P and Pocholle J P 1998 Compact Nd:YAG and Nd:YVO_4 amplifiers end-pumped by a high-brightness stacked array *IEEE J. Quantum Electron.* **34** 577–85
[16] van Druten N J, Oemrawsingh S S R, Lien Y, Serrat C, van Exter M P and Woerdman J P 2001 Observation of transverse modes in a microchip laser with combined gain and index guiding *J. Opt. Soc. Am. B-Opt. Phys.* **18** 1793–804
[17] Kemp A J, Conroy R S, Friel G J and Sinclair B D 1999 Guiding effects in Nd:YVO_4 microchip lasers operating well above threshold *IEEE J. Quantum Electron.* **35** 675–81
[18] Dong J, He Y, Bai S C, Ueda K I and Kaminskii A A 2016 A Cr^{4+}:YAG passively Q-switched Nd:YVO_4 microchip laser for controllable high-order Hermite-Gaussian modes *Laser Phys.* **26** 095004
[19] Chen Y F 2000 Pump-to-mode size ratio dependence of thermal loading in diode-end-pumped solid-state lasers *J. Opt. Soc. Am. B-Opt. Phys.* **17** 1835–40
[20] Ma J, Dong J, Ueda K and Kaminskii A A 2011 Optimization of Yb:YAG/Cr^{4+}:YAG composite ceramics passively Q-switched microchip lasers *Appl. Phys. B-Lasers Opt.* **105** 749–60